Fish and Shellfish Immunology 87 (2019) 166–177

Contents lists available at ScienceDirect

Fish and Shellfish Immunology

journal homepage: www.elsevier.com/locate/fsi

Full length article

Innate immune responses and metabolic alterations of mud crab (*Scylla paramamosain*) in response to *Vibrio parahaemolyticus* infection

Xusheng Zhang[a,b,c,1], Xixiang Tang[d,1], Ngoc Tuan Tran[a,b,c], Ying Huang[a,b], Yi Gong[a,b,c], Yueling Zhang[a,b,c], Huaiping Zheng[a,b,c], Hongyu Ma[a,b,c], Shengkang Li[a,b,c,*]

[a] Guangdong Provincial Key Laboratory of Marine Biology, Shantou University, Shantou, 515063, China
[b] Marine Biology Institute, Shantou University, Shantou, 515063, China
[c] STU-UMT Joint Shellfish Research Laboratory, Shantou University, Shantou, 515063, China
[d] Key Laboratory of Marine Genetic Resources, Third Institute of Oceanography, Ministry of Natural Resources, Xiamen, 361005, China

ARTICLE INFO

Keywords:
Immune responses
Scylla paramamosain
Metabolomic
ATP
Microbial abundant
Hemocyte

ABSTRACT

Vibrio parahaemolyticus is one of the major pathogens caused diseases in cultured mud crab (*Scylla paramamosain*). Mud crabs lack an adaptive immune system, their defenses depend almost on innate immunity. Evaluation of the molecular responses of mud crabs to pathogens is essential for control of disease occurrence in farmed animals. In this study, the impacts of *V. parahaemolyticus* on immunity-related genes and metabolites in mud crabs of different groups (PG, SG and MG refer to controlled, survival and moribund groups, respectively) were investigated. Our results revealed that *V. parahaemolyticus* infection stimulated significant expressions of immune-related genes (prophenoloxidase, alpha 2-macroglobulin, lysosomal-associated membrane protein, Rab5, C-type lectin B and anti-lipopolysaccharide factor 5) in the MG within 72 h post-infection. The ATP content was significantly reduced in all tissues except muscle of moribund mud crabs. A total of 668 metabolites (including 190 down-regulated and 145 up-regulated) were identified and assigned to 77 pathways in both SG and MG. Metabolites involved in the saturated fatty acid are up-regulated, whereas unsaturated fatty acid and amino acid metabolisms are down-regulated in the immune system of mud crabs during the bacterial infection in MG. Furthermore, a reduction of hemocyte number and an increase of microbial abundance was found in MG. Our results demonstrated that *V. parahaemolyticus* induced death of mud crabs through reducing the metabolites associate with energy biosynthesis and innate immune system (i.e. proliferation of hemocyte and melanization), resulting in decrease of ATP in different tissues and failed to clearance of pathogens, respectively. The findings of this study provide a basic information of the responses of mud crab on bacterial infection, which is essential for prevention and control of diseases in mud crab aquaculture.

1. Introduction

In southern China, mud crab (*Scylla paramamosain*) is one of the most important commercial mariculture species [1]. Under culture condition, the mud crabs are usually infected by *V. parahaemolyticus*, which is mainly responsible for disease outbreaks and have caused large economic losses of mud crab production in China [2]. However, it is difficult to prevent the spread of *V. parahaemolyticus* due to poor understanding about their infection mechanism associate with host, thus more investigations need to carry out in this field.

Similar to other invertebrates, mud crabs lack an adaptive immune system and their defense depends entirely on innate immunity as primary mechanisms of protection against invading pathogens [3]. Once pathogens have infected the host, they activate the host's immune system by stimulating the activities of antimicrobial peptides, C-type lectins (CTLs), inflammatory factors, and pattern-recognition receptors (PRRs) in host cells [4–7]. Moreover, the activation of immune system will increase the ATP requirements. For example, the Na−K-ATPase can convert the free energy of ATP into transmembrane ion gradients, and then induced changes in the intracellular calcium ion concentrations, which affect the activity of immune protein, such as C-type lectins, calcium vector and calmodulin [5,8–11]. However, the alteration in immune gene and protein levels might not directly relate to phenotypes. In most cases, metabolites are downstream functional molecular

* Corresponding author. Guangdong Provincial Key Laboratory of Marine Biology, Shantou University, Shantou, 515063, China.
E-mail address: lisk@stu.edu.cn (S. Li).
[1] These authors contributed equally to this paper.

https://doi.org/10.1016/j.fsi.2019.01.011
Received 10 November 2018; Received in revised form 7 January 2019; Accepted 8 January 2019
Available online 09 January 2019

of genes and proteins [12]. Currently, our understanding on the metabolic response of mud crabs against *V. parahaemolyticus* is still vague.

In contrast to traditional methods that detect the metabolite changes during a specific biological process, mass spectrometry-based metabolome profiling is a new choice in systems biology approaches that provide a better comprehension of the complex biological systems, enabling to measure all small molecules, chemicals, and metabolites present in a given sample [13]. These metabolomics approaches include targeted and the untargeted. A targeted approach, which can measure specific metabolites, is suitable for testing specific hypotheses, and the untargeted approaches that measure all detectable compounds are most often used for general scientific researches [14]. There are many techniques can be used to measured metabolites. In metabolomics, the primary analytical platforms include ^{1}H nuclear magnetic resonance (NMR) spectroscopy, liquid chromatography mass spectroscopy and (LC-MS) and gas chromatography mass spectroscopy and (GC-MS), that all of these platforms can measure metabolites comprehensively [13]. Comparison among these platforms, liquid chromatography-mass spectrometry (LC-MS) shown many advantages. For example, it is sensitive to low concentration of metabolites and has good coverage of mass range that allow to measure metabolites with different chemical properties, thus, it can simultaneously detect watery and lipid metabolites [15]. It is efficiently and widely used in medicine and biology [16,17], which measures different classes of metabolites within different kinds of samples [14], and provides an overall characterization of the metabolic mechanisms at molecular and cellular levels upon the stimulation of external factors [18]. In aquatic animals, LC-MS have been efficiently applied in study potential mechanism of disease [14]. In addition, the metabolites is directly exchanged between the plasma other organs as pervious reported [19]. Thus, Study of the changes of metabolites in the plasma can provide a whole-organism overview of physiological status of organisms.

In this study, we employ LC-MS untargeted to analyze the changes of metabolites in the plasma of mud crabs either survival or moribund after challenge with *V. parahaemolyticus*. The results of this study enhance our understanding of the mechanisms that showed the disease resistance-related roles of metabolites in mud crab after bacterial infection, which is essential for prevention and control of this disease in culture mud crabs.

2. Materials and methods

2.1. Mud crab, bacterial challenge and sample collection

A total of 110 healthy mud crabs (approximately 50 g each) were acclimatized in laboratory tanks (at salinity of 8‰ and temperature of 25 °C) for one week before further processing. The mud carbs were fed once daily (at dusk) with fresh bivalve mollusks. During the acclimatization period, water was exchanged daily. After a 1-week of acclimatization, 40 crabs were collected and divided into four groups of ten. For the pilot trial infection, each crab was injected with 100 μL of *V. parahemolyticus* suspension (at one of different concentrations of 1×10^6, 1×10^7, 1×10^8, and 1×10^9 cells/mL) at the base of the fourth leg. The desired concentrations of *V. parahemolyticus* were adjusted using a hemocytometer-based cell counting method. In the control, crabs were injected with the same volume of sterile phosphate-buffered saline solution (1 × PBS, Sangon Biotech, Shanghai, China). The experiments were conducted under the laboratory conditions for one week with daily removal of mortalities. At the termination, the survival rate was noted, calculated and analyzed using GraphPad Prism 5 software.

In the main infection trial, 80 mud crabs were randomly distributed into groups of 20 crabs in 4 separate tanks. Mud crabs in three tanks (experimental group) were injected with 100 μL (1×10^7 cells) of *V. parahemolyticus* while mud crabs in remaining tank (control group) were injected with 100 μL 1 × PBS. The mud crabs were observed for 72 h. At termination the mud crabs in control and experimental tanks were correspondingly divided into PBS (PG) and moribund (MG) and survival (SG) groups (both later groups were clarified depending on crab health status). Hemolymph (400 μL) was withdrawn from each crab (at least six crabs/group) using a disposable syringe (1 mL) before (0 h post infection-hpi) and at 72 hpi with *V. parahemolyticus*. The samples were stored in 0.5 mL-tubes containing either ice-cold acid citrate dextrose (ACD) anticoagulant buffer (1.32% sodium citrate, 0.48% citric acid, and 1.47% glucose) [20] (used for RNA extraction) or EDTA (used for LC-MS analysis). The hemolymph samples were immediately centrifuged at $3000 \times g$ for 10 min at 4 °C to collect the plasma, then stored at −80 °C for further uses. Other tissues, including muscle, brain, gill, plasma, hemocytes, hemopoietic tissue, and heart, were quickly collected, rinsed with 1 × PBS and put into liquid nitrogen immediately, which used for ATP assay.

2.2. Quantitative RT-PCR for the expression of immunity-related genes

Total RNA from hemocytes was extracted using DNA/RNA Isolation kits (Omega, USA) following the manufacturer's instructions. cDNA library was synthesized using PrimeScript RT reagent Kit with gDNA Eraser (Takara, Dalian, China) following the manufacturer's instructions, serially diluted four-fold and used as the template for qRT-PCR. Six innate immune-related genes, including prophenoloxidase (proPO), alpha 2-macroglobulin (α-2m), lysosomal-associated membrane protein (Lamp), Rab5, C-type lectin B (CTL-B) and anti-lipopolysaccharide factor 5 (Alf5) were used for investigation. β-actin was used as an internal control gene. qRT-PCR was carried out with SYBR® Premix Ex Taq™ II Kit (Takara, Dalian, China) in LightCycler® 480 (Roche, USA). The total reaction volume of 20 mL contained 10 mL of SYBR® Premix Ex Taq™ II, 2 mL of cDNA, 0.8 mL (10 mM) of each (forward and reverse) primer (Table 1), and 6.4 mL of ultra-pure water. The amplification procedure was as followed: a denaturation step of 95 °C for 30 s, followed by 40 cycles of 95 °C for 5 s, 60 °C for 20s, and a melting curve analysis from 65 °C to 95 °C. Each sample was done in triplicate. The efficiency of the amplification was tested. Data were analyzed with the LightCycler 480 software (Roche, USA). The relative transcript levels of genes were determined using the $2^{-\Delta\Delta\ Ct}$ algorithm with an internal control (β-actin). All data were expressed as means ± SD. The data were subjected to one-way ANOVA analysis using OriginPro8.5 and GraphPad Prism 5 statistical software followed by *t*-test, and the levels of significant differences was set at $P < 0.05$, $P < 0.01$, and $P < 0.001$.

2.3. UPLC-MS analysis

A total of 400 μL of plasma was mixed with methanol, vigorously

Table 1
Sequences of primers used in this study.

Primers	Sequence (5′ to 3′)
RT-PCR	
Lamp-F	CTATCGCTGTTGGATGTGCTCTGG
Lamp-R	GATTGATACGCTCCCGACCTCC
Rab5-F	GCTGCTTGGGGAGTCTGCTGTG
Rab5-R	CATACAGTCTGGGTCAGGAAGGC
β-actin-F	GCGGCAGTGGTCATCTCCT
β-actin-R	GCCCTTCCTCACGCTATCCT
Alf5-F	CTTGAAGGGACGAGGTGATGAG
Alf5-R	TGACCAGCCCATTCGCTACAG
α2m-F	ATGACAGGCGATGGATGCG
α2m-R	GGGATGTAACCCGAAATGAGG
CTL-B—F	GGGACAGACGAAGTAATGGACGG
CTL-B-R	ATTTTGGGTTGGGGAGGCACAG
proPO-F	AGCGAACAGAAGCAAGTG
proPO-R	AGCGAACAGAAGCAAGTG

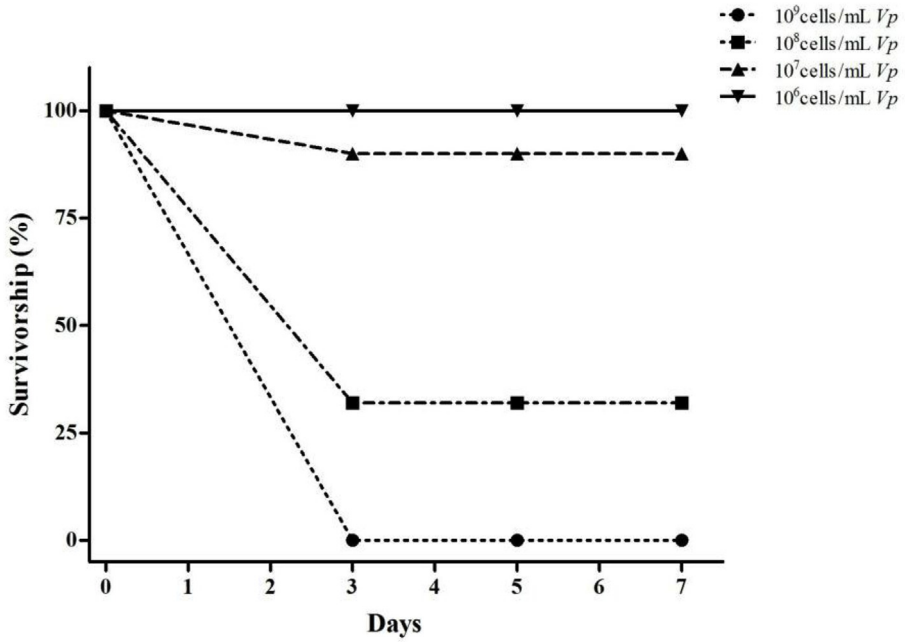

Fig. 1. Survival curves of the crabs for different concentrate of *V. parahaemolyticus* infection.

shaken for 30 s and allowed to stand at 4 °C for 5 min. After centrifugation (12,000 × *g* at 4 °C for 15 min), the supernatant was loaded for the analysis performing Agilent 1290 Infinity LC System (Agilent Technologies, Germany) and ACQUITY UPLC BEH Amide reverse-phase column (2.1 mm id × 100 mm × 1.7 μm) (Waters, USA). After loading, the sample was filtered and centrifuged to remove the particle. The mixture of 25 mM of acetic acid and 25 mM of ammonia water and acetonitrile were used in the mobile phases: A and B, respectively. The elution was eluted with 5% A–95% B for 0.5 min, 35% A–65% B for 6.5 min, 60% A–40% B for 2 min, and then eluted with 5% A–95% B for 3.5 min to balance the column. The total chromatographic elution process was 12 min, with the flow rate of 500 μL/min.

AB 5600 Triple TOF mass spectrometer system (AB Sciex, USA) was regulated by Analyst TF 1.7 software to screen molecule and ion > 100 and collect secondary mass spectrometric data. The ProteoWizard software was used for raw peak exacting, data baseline filtering and calibration, peak alignment, peak identification, and peak area integration. PCA showed the distribution of origin data. A supervised OPLS-DA was applied to obtain a high level of group separation and to enhance our understanding of the variables responsible for classification. KEGG were used to search for the pathways of metabolites. The difference metabolites were identified based on the following principles: the theoretical fragments should exhibit three strong peaks matching with the secondary characteristic fragments and should be able to cover more than 80% of secondary characteristic fragments. Significant differences ($P < 0.05$) of each variable were first detected using the *t*-test; the only metabolite with $P < 0.05$ was considered for subsequent analyses.

2.4. ATP assay

ATP concentrations were tested using an enhanced ATP Assay Kit (Beyotime, Shanghai, China) according to the manufacturer's protocol. Tissues or cells were lysed with ATP lysis buffer (containing 200 μL of lysate per 2 mL or 0.2 mg) after vortexed with ceramic beads and centrifuged at 12,000 × *g* for 5–10 min at 4 °C. The supernatant was collected and stored on ice. Before the ATP test, 100 μL of ATP working solution (ATP test solution: ATP test dilution = 1:4) was added to 96-well ELISA plates and incubated for 3–5 min at room temperature. Next, a 20-μL of the supernatant was transferred to 100 μL of ATP working solution, mixed quickly, and the amount of luminescence emitted was immediately measured using a microplate reader (Promega, BioTek, USA). The luminescence data were normalized to ATP amounts; all data were expressed as means ± SD. Differences between groups were analyzed by *t*-test using GraphPad Prism 5, and the levels of significant differences was set at $P < 0.05$, $P < 0.01$, and $P < 0.001$.

2.5. Count of microbial cells and hemocytes

The enumeration of microbial cells and hemocytes in the hemolymph of crabs was performed according to a method developed by our laboratory members [21]. Briefly, the hemolymph-anticoagulant mixture was passed through a sterile filter (Millipore, Germany) with a 5 μm mesh membrane, and the filtrate was collected in a new 5 mL centrifuge tube. The microbial cells in the filtrate were fixed with an equal volume of sterile formalin solution (containing 20 g/L NaCl and 30 mL/L formalin) for 30 min. The mixture was filtered through a sterile filter (Millipore, Germany) with a 0.2-μm mesh membrane. Both hemocytes (on the 5 μm mesh membrane) and microbial cells (on the 0.2 μm mesh membrane) were stained with SYBR® Green I solution (1:40 v/v SYBR® Green I in 1 × Tris-EDTA buffer) for 20 min. The stain solution was removed; the membrane was placed on a glass slide adding 25 μL sterile glycerine (10% v/v). Cells were counted at 1000 × magnification using a fluorescence microscope (Zeiss, Germany) with a blue filter set. Each sample was extracted and counted in triplicates.

3. Results

3.1. Crabs survival upon V. parahaemolyticus infection

Survival of mud crabs challenged with *V. parahaemolyticus* was tracked for 7 days (Fig. 1). Survival was bacterial concentration-dependent, with 100% survival at 100 μL of lowest bacterial concentration (10^6 cells/mL), 90% at 10^7 cells/mL, 30% at 10^8 cells/mL, and 0% at 10^9 cells/mL. Thus, 100 μL of *V. parahaemolyticus* at 10^8 cells/mL was used for further experiments.

3.2. Relative expression of immunity-related genes

In order to study the innate immunity system of mud crabs in

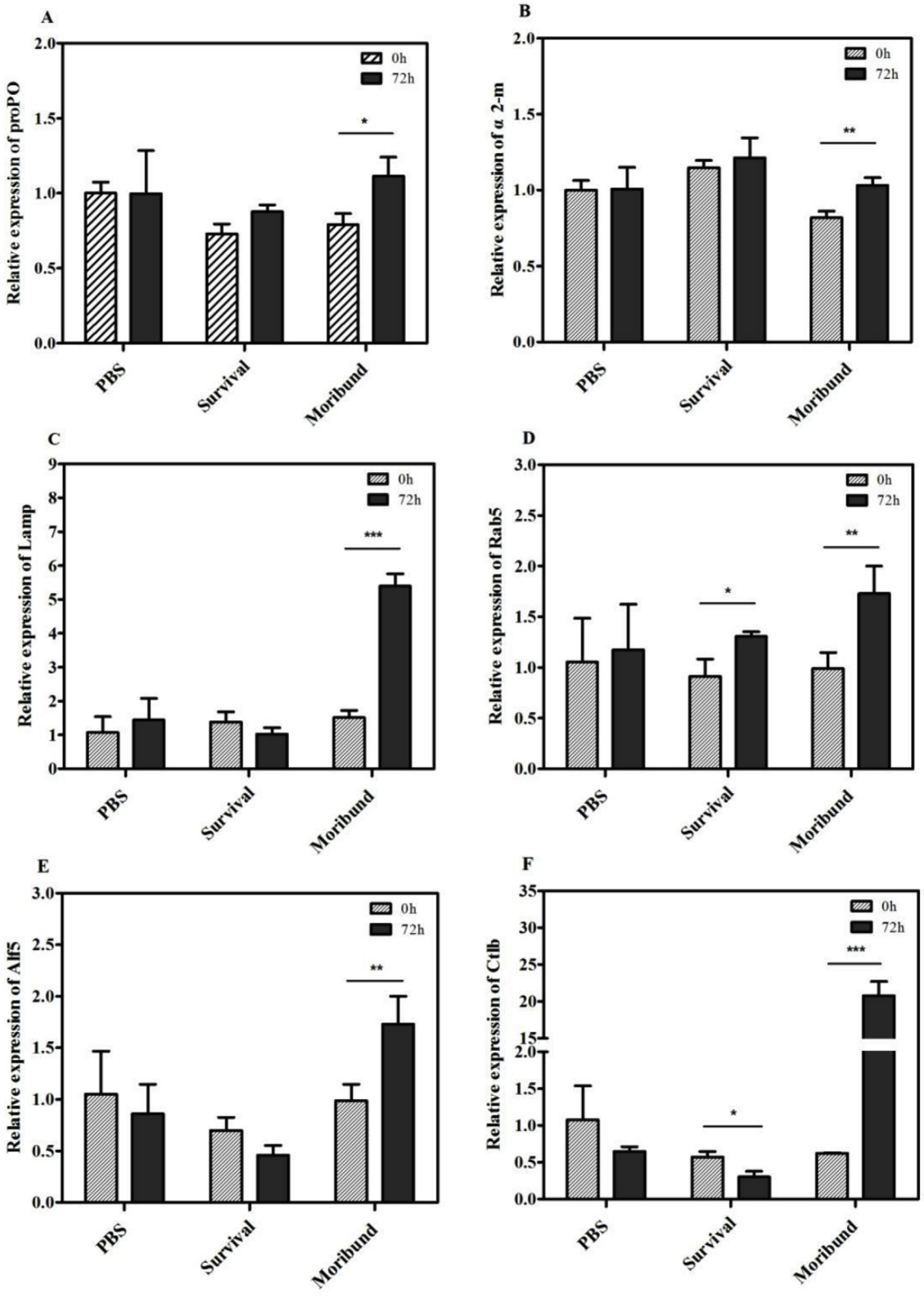

Fig. 2. Immune genes expression profiles.

(A) and (B) represented proPO and α2-macroglobulin expression in the mud crabs hemocyte after *V. parahaemolyticus* challenge. (C) and (D) represented Lamp and Rab5 expression in the mud crabs hemocyte after *V. parahaemolyticus* challenge. (E) and (F) represented Alf5 and Ctlb expression in the mud crabs hemocyte after *V. parahaemolyticus* challenge. At least six crabs were used in each group. Error bars represent ± SD of three independent repeats. Asterisks indicate significant differences (*$P < 0.05$, **$P < 0.01$, ***$P < 0.001$) analyzed by *t*-test.

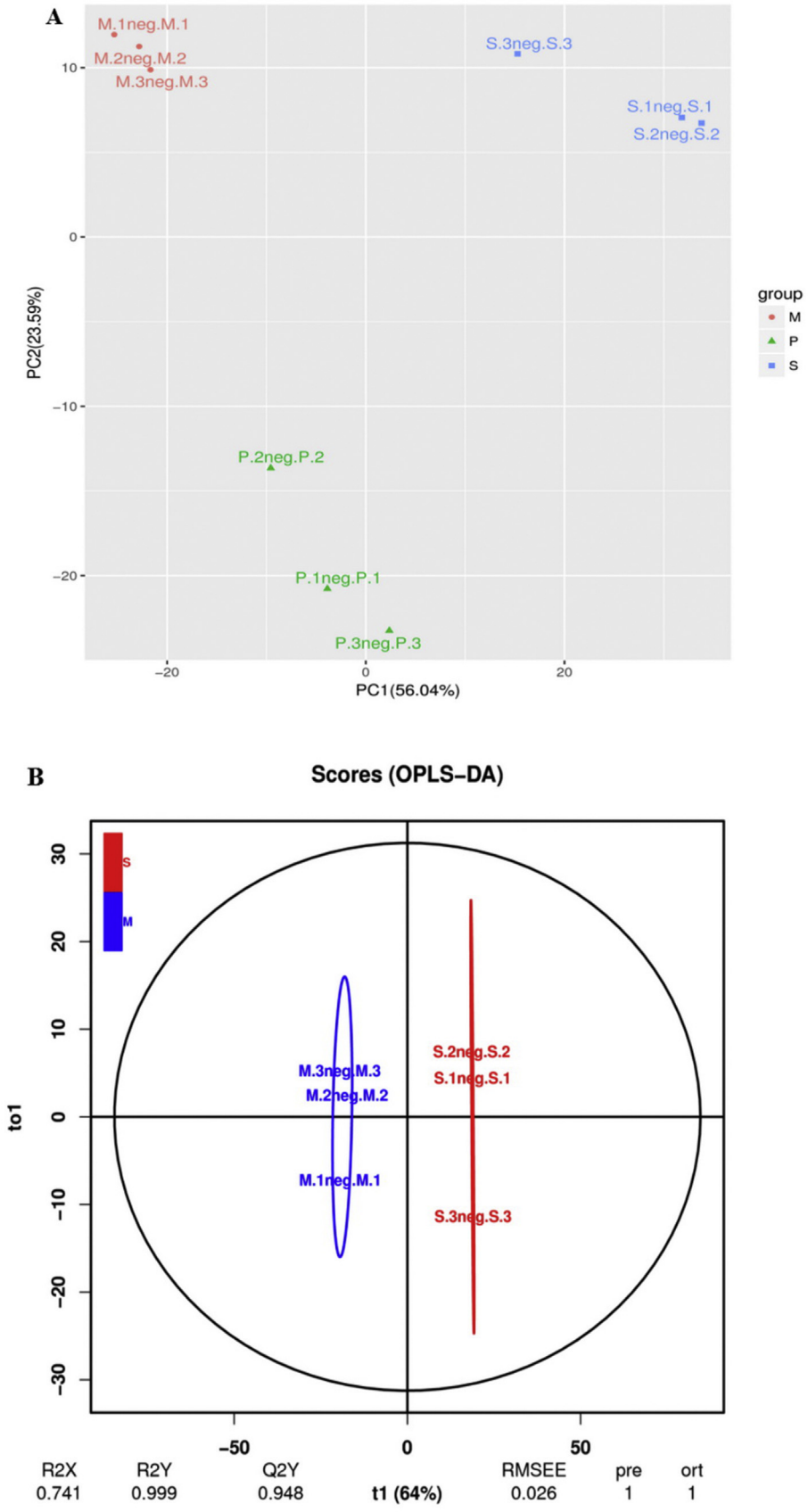

Fig. 3. PCA and OPLS-DA score plots derived from the UPLC-MS metabolite profiles of plasma.
(A) PCA score plot of PBS group (green triangles), moribund group (red circles) and survival group (blue squares). (B) OPLS-DA score plot of moribund group and survival group. (For interpretation of the references to colour in this figure legend, the reader is referred to the Web version of this article.)

experimental groups in response to the *V. parahaemolyticus* infection, six of the genes that are associated with immune-related pathways such as prophenoloxidase system (proPO and α-2m), hemocyte endocytosis (Lamp and Rab5), and immune factors (CTL-B and Alf5), were selected to investigated using qRT-PCR (Fig. 2). The results revealed that the genes were expressed differently either between SG and MG (at 0 hpi) or between these groups and PBS (at 72 hpi). Compared with the controls (at 0 hpi), a significant up-regulation in all investigated genes was found in MG (at 72 hpi, $P < 0.05$). In SG, with the exception of Rab5 and CTL-B, which were significantly up- and down-regulated at 72 hpi, respectively ($P < 0.05$), the expression of all remaining genes did not express significantly in comparison with those at 0 hpi ($P > 0.05$).

3.3. Metabolic profiling of plasma

A principal component analysis (PCA) was used to study cross changes in the metabolic physiology of mud crabs in experimental groups. A plot based on PCA scores showed a significant separation of metabolite profiles in the plasma among groups (PG, MG, and SG) (Fig. 3A). Orthogonal projections to latent structures-discriminant analysis (OPLS-DA) revealed a clear discrimination in the metabolic variation between SG and MG (student *t*-test, $P < 0.05$) (Fig. 3B) (which was verified based on the calculated parameters of $R^2X = 0.741$, $R^2Y = 0.999$, and $Q^2 = 0.948$).

Using OPLS-DA analysis (student *t*-test, $P < 0.05$ and VIP > 1), a total of 668 metabolites in both SG and MG were identified; of which, 190 were down-regulated, 145 were up-regulated, and 333 were unchanged in MG. A total of 169 metabolites were annotated to 50 metabolic pathways (Supplementary Fig. S1A). Among these metabolites, 17 and 117 metabolites were found to be related to diseases and physiological metabolism, respectively. Similarly, 17 and 92 metabolites related to diseases and physiological metabolism, respectively, were obtained in MG and PG (Supplementary Fig. S1B). However, the different metabolites present in both PG and SG were only annotated to 28 metabolic pathways; only 2 metabolites were related to diseases and 37 metabolites were to metabolism (Supplementary Fig. S1C). To further integrate the different metabolites into key metabolic pathways of both SG and MG, a number of 33 metabolites was picked out; among these screened metabolites, 12 metabolites were classified to be amino acids and analogues, five were organic acids, seven were lipid metabolites and ten were 'others' (Table 2).

3.4. Characterization and functional analysis of key metabolic pathways

In the KEGG annotation, 17 metabolites were assigned to the "energy metabolism" pathway (Fig. 4). The metabolites, including DL-lactate, L-carnitine, acetylcarnitine, proline, hydroxyproline, argininosuccinic acid, and malate, were found to be higher in SG compared with that in MG.

Compared with the obtained metabolites in MG, a higher level of metabolites associated with fatty acid and amino acid metabolisms was observed in SG (Fig. 5). The arachidonic and eicosapentaenoic acids were down-regulated in the unsaturated fatty acids metabolism present in the MG (Fig. 5A). On the contrary, myristic acid, palmitic acid, stearic acid, and 9(S)−HODE (producing stearic acid) were up-regulated in the saturated fatty acids metabolism (Fig. 5B).

All amino acids were down-regulated in MG such as arginine, proline, methionine, taurine, glutamine, hydroxyproline, phosphoserine, tyrosine, phenylalanine and leucine. The second messenger (like cGMP) is tightly connected to amino acid metabolism, which was found to be up-regulated in MG. Other metabolites, i.e. uric acid, inosine, cysteinesulfinic acid, were down-regulated in MG (Fig. 5C).

Table 2
Identification of significantly different metabolites in plasma between the moribund (MG) and the survival (SG) crabs after infection with *V. parahaemolyticus*.

Metabolites	Fold change	P-value	VIP	regulated
DL-lactate	0.373	0.009	1.163	down
L-Proline	0.292	0.001	1.222	down
Taurine	0.372	0.017	1.168	down
Hydroxyproline	0.289	0.010	1.213	down
L-Leucine	0.300	0.002	1.242	down
L-Malic acid	0.253	0.003	1.210	down
L-Glutamine	0.576	0.017	1.193	down
L-Methionine	0.496	0.002	1.236	down
Xanthine	0.131	0.020	1.160	down
L-Cysteinesulfinic acid	0.110	0.002	1.233	down
L-Phenylalanine	0.242	0.014	1.208	down
L-Arginine	0.345	0.025	1.167	down
L-Tyrosine	0.576	0.004	1.200	down
Acetylcarnitine	0.127	0.001	1.240	down
L-Carnitine	0.201	0.006	1.189	down
Acadesine	0.448	0.013	1.192	down
3-Phosphoserine	0.178	0.001	1.248	down
Inosine	0.068	0.000	1.247	down
Glutamyl Glutamine	0.350	0.006	1.211	down
Argininosuccinic acid	0.255	0.001	1.211	down
Eicosapentaenoic acid	0.741	0.041	1.064	down
Arachidonic Acid	0.478	0.003	1.246	down
Uric acid	0.171	0.008	1.180	down
Ganoderic acid	0.043	0.037	1.172	down
Quercetin	1.744	0.039	1.144	up
Rofecoxib	1.532	0.008	1.201	up
9(S)−HODE	2.748	0.012	1.201	up
Embelin	1.542	0.005	1.225	up
Myristic acid	2.118	0.001	1.226	up
Palmitic acid	1.897	0.001	1.229	up
Stearic acid	1.686	0.034	1.119	up
Cyclic guanosine monophosphate	1.232	0.007	1.169	up
Pristanic acid	3.590	0.000	1.253	up

3.5. Variation of ATP content in different tissues

The results showed that ATP content significantly decreased in all tissues examined, including brain (4.32-fold), heart (28.88-fold), gill (5.70-fold), hemopoietic tissue (3.20-fold), plasma (21.21-fold) and hemocyte (16.78-fold), with the exception of that in muscle, in the MG in comparison with the SG (Fig. 6). In comparison to the PG, SG had a 10.11-fold decrease of ATP levels in the brain, a 4.24-fold decrease of that in hemocyte, and a 1.78-fold decrease of that in plasma, but not in other tissues.

3.6. The number of microbial cells and hemocytes in hemolymph

The number of microbial cells in the hemolymph of mud crab in both MG and SG increased to 2.2×10^5 and 4.5×10^4 cells/mL after 72 hpi of *V. parahaemolyticus* compared with initial inoculum (0 hpi), which was 5.8×10^4 and 4.5×10^4 cells/mL, respectively (Fig. 7A). In contrast, the number of hemocytes of both MG and SG decreased, with counts ranging from 4.6×10^6 cells/mL (at 0 hpi) to 1.1×10^6 cells/mL (at 72 hpi) and 1.0×10^7 cells/mL (at 0 hpi) to 3.0×10^6 cells/mL (at 72 hpi), respectively (Fig. 7B).

4. Discussions

Numerous pathogens threaten the survival of organism across the world [22], they have caused an outbreak of diseases to host including vertebrates and invertebrates [23,24]. As a member of invertebrate, mud crab is usually infected by several pathogens, which cause enormous economic losses in aquaculture production [2,25]. The previous studies have shown that *V. parahaemolyticus* infection caused diseases in cultured mud crabs, leading to high mortality rate in mud crab

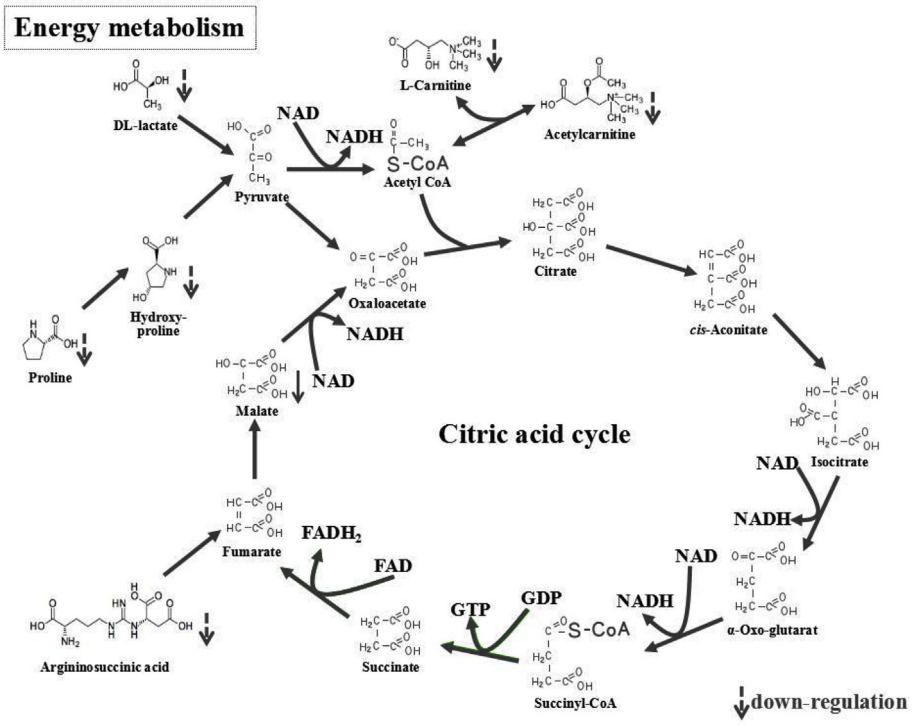

Fig. 4. Different metabolites relevant to citric acid cycle for ATP producing during MG vs SG.

populations [2]. Obviously, previous reports have confirmed the impacts of pathogenic infection to changes in metabolisms of the host [12]. However, metabolic changes in mud crab due to *V. parahaemolyticus* infection is still unknown. In this study, the expression of multiple genes associated with the innate immune response and metabolic profiles of plasma of mud crabs after challenge with *V. parahaemolyticus* were fully investigated for the first time. This research found that some metabolites are engaged in the immune system of mud crabs during the bacterial infection. Our study found that the mortality rate of mud crab is dose-dependent in respond to *V. parahaemolyticus*. This result is agreed with the results from previous studies [26], indicate that a *V. parahaemolyticus* outbreak will cause mass deaths of mud crabs and enormous economic losses in aquaculture.

In invertebrates, innate immune system is activated by pathogens to inhibit infection, including melanization (proPO and α-2m), phagocytosis (Lamp and Rab5), and immune factor (CTL-B and ALF5) [3,5,20,27,28]. In this study, we found the up-regulation of proPO, α-2m, Lamp, Rab5, CTL-B, and Alf5 in MG after challenge with *V. parahaemolyticus*. This is similar to the results of previous studies [5,20], which the authors also confirmed the same expression trend of these genes in crabs in responding to the infection of *V. parahaemolyticus*. This result indicated the immune system is activated after infection of *V. parahaemolyticus* in MG. Furthermore, our study revealed that immune genes were up-regulated in MG, which is consistent with the case of moribund striped bass (*Morone saxatilis*) [29]. Whereas, in the survival group, Rab5 was significantly up-regulated ($P < 0.001$), while CTL-B significantly down-regulated ($P < 0.05$). As pervious study [5,20], Rab5 and CTL-B are activated to clearance of pathogen in marine organism, but the CTL-B is decline in later stage comparison to early stage of infection, this partly explain the above result. These suggest that both Rab5 and CTL-B may play crucial role in mud crab protecting against the infection of *V. parahaemolyticus*; however, the molecular mechanisms should be confirmed in further investigation. Thus, our results indicate that the pathogen *V. parahaemolyticus* activated the innate immune system of mud crabs through the modulation of expression of genes, which agrees with the conclusion in previous study [3,5,20].

Previous studies have revealed changes in levels of immune-related components associated with the physiological metabolism changes [13]. For example, the amino acid and energy metabolism was disturbed post pathogen infection in *Portunus trituberculatus* [12]. In this study, UPLC-MS-based metabolomics analysis was performed to determine difference in metabolites and metabolism-related pathways in the plasma of mud crabs in MG and SG. UPLC-MS-based metabolomics has a good coverage of mass range and allow to measure metabolites with different chemical properties. It is common to use for exploring the potential mechanism of disease and obtain a whole-organism overview of the affected metabolites to reflect the variation of physiology [16,30]. In our study, the different metabolites between MG and SG were integrated into four key metabolic pathways, including energy metabolism, unsaturated fatty acid, saturated fatty acid and amino acid metabolism. Consistent with this observation, energy metabolism and amino acid metabolism have been found in *P. trituberculatus* post *Vibrio alginolyticus* infection [12]. These results suggested the significance of these physiology metabolisms in their host upon stimulation of pathogens.

In the energy metabolism, the plasma TCA cycle-related metabolites were down-regulated in MG, indicating that the substrates provided from different tissues were not enough for the TCA cycle to produce ATP via respiratory electron-transport chain. This was also verified by the lowest ATP content found in all tissues, excepting muscle, of the moribund mud crabs. The low ATP content inhibits the production of energy to maintain a normal physiological activity of the organism. The results of this study revealed that when the ATP content declined in the hemopoietic tissue of moribund mud crab may lead to a decrease in the proliferation of hemocytes and amount of hemocytes (which was lower than their survival counterparts). This is consistent with previous report [31] that the cell proliferation needs to expend the ATP as a substrate. Also, a decrease in ATP content in the heart may be related to the functions decline, which might explain the reasons for the death in moribund mud crab after bacterial infection [32]. In contrast, in the survival mud crab, the ATP content was not significantly varied during the challenge test, indicating the sustainably normal physiology activities occurring in these individuals. Interestingly, ATP content was slightly increased in the muscle of moribund mud crabs, which is

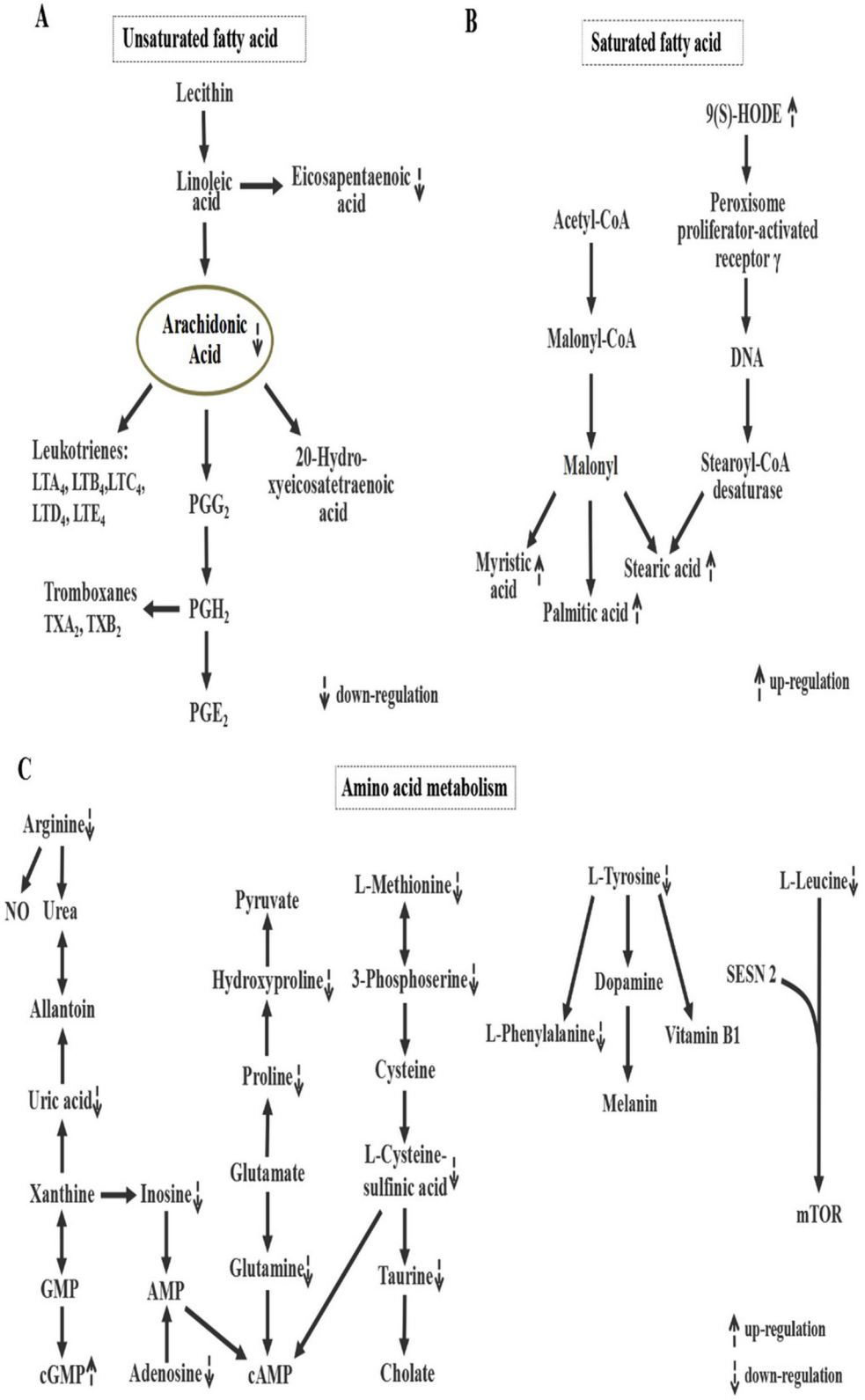

Fig. 5. Different metabolites involved in metabolic pathways.
Different metabolites relevant to unsaturated fatty acid (A), saturated fatty acid (B), and amino acid (C) metabolic pathways.

similar to that in a previous report [33], where the maximal activities of skeletal muscle transition increased respiration rate and ATP consumption. Thus, it is inferred that the survival and PG mud crabs were more active in the usage of ATP than their moribund counterparts.

In the unsaturated fatty acid metabolism, arachidonic acid was decreased in MG, this might be the decrease in the appetite of infected mud crabs associated with the health status [30]. Actually, arachidonic acid is known to be substrates for the biosynthesis of prostaglandin, thromboxane A2 and leukotrienes, which have been previously reported involving in the risks influencing growth performance,

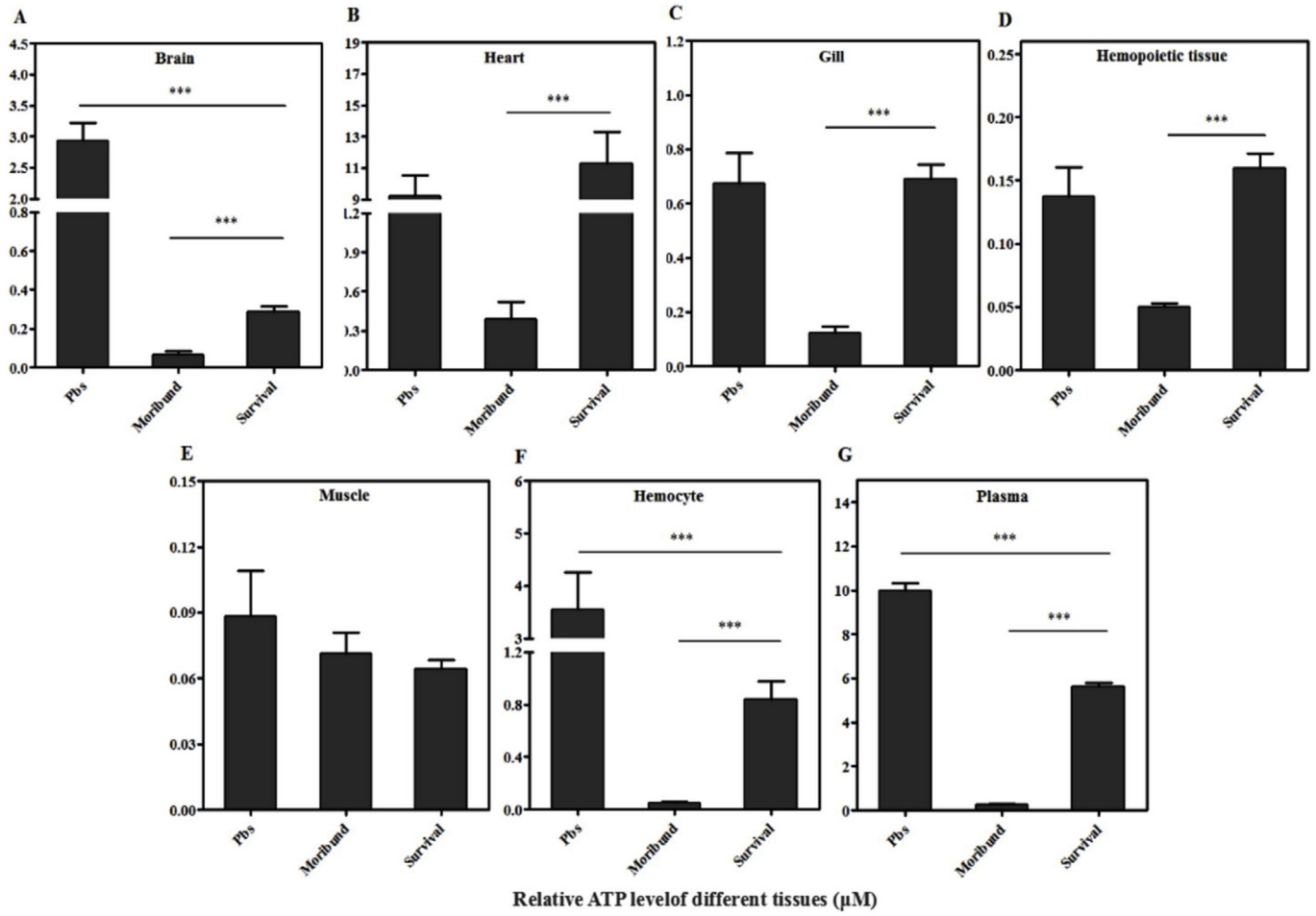

Fig. 6. ATP content in different tissues.

ATP content of brain (A), heart (B), gill (C), hemopoietic tissue (D), muscle (E), hemocyte (F), plasma (G) of PBS group, survival group and moribund group were measured by using a microplate reader. At least six crabs were used in each group. Error bars represent ± SD of three independent repeats. Asterisks indicate significant differences (*$P < 0.05$, **$P < 0.01$, ***$P < 0.001$) analyzed by *t*-test.

development, antioxidant activity, and immune responses in human and aquatic animals [34–37], as well as promoting blood agglutination activities [38]. Herein, the decrease in levels of arachidonic acid in moribund mud crabs may directly affect the physiological responses (including immune responses) in the host. Furthermore, the levels of eicosapentaenoic acid were found to be decreased in MG compared with that in SG or PG. It has been known that eicosapentaenoic acid involved in the unsaturated fatty acid metabolism plays important roles in exhibiting antibacterial activity against bacteria (especially Gram-positive bacteria) [39,40]. These results indicated the different metabolites related to unsaturated fatty acid metabolism are closely related to immune activation, cell proliferation, apoptosis, and bacteria clearance of organisms. Therefore, we proposed that the lower level of unsaturated fatty acid may decline the resistant ability, and then make them dead after disease infection.

In the saturated fatty acid metabolism, it was found that the myristic acid, palmitic acid and stearic acid were increased in MG, inferring the inadequate saturated fatty acid supply during the infectious period of moribund mud crabs [30]. Previous studies have confirmed the association of levels of saturated fatty acids with an increase in cardiovascular disease-related mortality [41], and an induction of apoptosis (by iron depletion) [42], lipotoxic impairment and cell death [43,44]. Of which, stearic acid, produced by the unsaturated fatty acid 9(S)−HODE (α-Dimorphecolic acid) *via* stimulating peroxisome proliferator-activated receptor γ induces stearoyl-CoA desaturase activity, is an antagonist of the leukotriene B4 receptor and inhibits the pro-inflammatory responses [45,46]. Thus, the robust of saturated fatty acids in MG suggested the involvement in an increase of the risk of cardiac dysfunction and induction of apoptosis in mud crab after *V. parahaemolyticus* infection.

Interestingly, as for amino acid metabolism, the metabolites (such as glutamine, inosine, adenosine, methionine, 3-phosphoserine and cysteinesulfinic acid) used for the cAMP synthesis were decreased in the moribund mud crabs, but such used for cGMP was increased. Previously, both cAMP and cGMP have been reported to serve as second messengers that are oppositely effective on the physiological metabolisms, including cardiac function, cell proliferation, chloridion and calcium ion flux [47–50]. Chloridion is known to be an important molecular that involved in the innate immunity of hosts [51]. The calcium ion flux that is affected either by cAMP, increasing the inflow of heart cells and stimulating the increase of cardiac contraction, or by cGMP decreasing the cardiac contraction [48]. In addition, some of the immunological proteins are activated by Ca^{2+}-dependent manner like C-type lectins, calcium-binding proteins and calmodulin [5,10,11]. Furthermore, the previous study has reported that both cAMP and cGMP are functional antagonists in the macromolecule permeability [52]. Thus, the down-regulated substrates directly affect the synthesis of cAMP, decline of cardiac function, inhibition of immune responses, iron influxes, and macromolecule transports. However, the upregulation of substrates used in the cGMP suppresses the function of cAMP via the protein kinase A hydrolysis [48,49]. Additionally, other metabolites (i.e. arginine, uric acid, proline, hydroxyproline and taurine) were

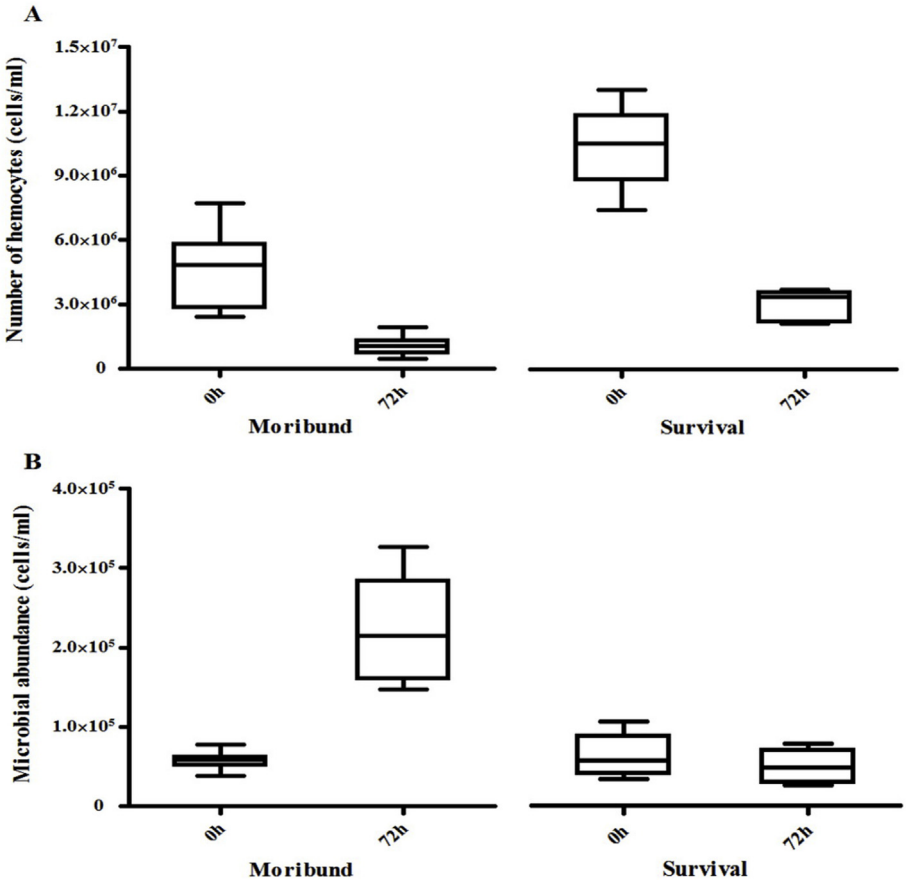

Fig. 7. The number of hemocyte and microbial abundant in hemolymph.
(A) The number of hemocyte in hemolymph of moribund group and survival group. (B) The microbial abundant in hemolymph of moribund group and survival group. Every group include six independent repeats. The boxes include the interquartile range (IQR), from the first and third quartiles, and the inside bold line represents the median. The dotted lines extending vertically from the boxes (whiskers) denote the lowest and highest values within 1.5 IQR from the first and third quartiles.

found to be down-regulated in MG. The results might be by the inhibition of the activation of inflammasome, clearance of pathogens, blood pressure, heart pulsation, cells proliferation, differentiation, calcium influx and accumulation were inhibited in cells in vivo [53–57]. A down-regulation of arginine, uric acid, and taurine in our study may imply a decrease in the production of NO, urea and cholate in MG, respectively, in the plasma of the host. This suggests an important role of these metabolites in the protection their host against pathogenicity, osmoregulation, and reducing oxidative impairment [58–60].

Furthermore, the two amino acids tyrosine and leucine were found to be down-regulated in the moribund mud crabs. Tyrosine can be converted into Vitamin B1 and dopamine that both have been reported to be associated with the cells differentiation, activation of immunity, melanization and apoptosis reduction via prevention of caspase 3 activated [61–63]. Leucine involves the mTOR pathway and regulates the cell proliferation via activating of sestrin-2 protein [64]. The decreased levels of these metabolites might be related to the decrease in the number of hemocytes and activities of immune components in moribund mud crabs compared with their survival counterparts. This is also verified by the reduction in hemocyte number and increase in microbial abundance in moribund mud crab. The hemocytes play important role in forming the primary line of host immune defense against infectious agents, and a decrease in the number of hemocytes lead to increase the presence of pathogens in the host [65]. This is in accordance with the findings in our study that the decrease in the number of hemocytes and inhibition of immune activities lead to an increase in microbial abundance. Moreover, the analysis of metabolic pathways showed an association among an improvement of microbial abundance and variation of metabolites and disease outbreaks and physiological metabolism changes (Supplementary Fig. S1).

In conclusion, the results of this study pointed out that *V. parahaemolyticus* was found to cause mortality in mud crabs after inoculation in a dose-dependent manner. The expression of immune-related genes, proPO, α-2m, Lamp, Rab5, CTL-B, and Alf5, in mud crabs after challenge with *V. parahaemolyticus*, indicating the important roles of them in the mud crab innate immune system. Moreover, the results of this study indicated that mud crabs consumed more ATP for the up-regulation of immune-related genes. The number of hemocytes was found to be inversely associated with the abundance of microbes in moribund mud crabs. Furthermore, some metabolites involved in the unsaturated fatty acid, saturated fatty acid and amino acid metabolisms are engaged in the immune system of mud crabs during the bacterial infection; however, further research is required to investigate the outcomes of this study, especially focusing on the metabolites related to immune metabolism. However, in the SG, the metabolism homeostasis seemed to stably maintain during the infection period. The findings of this study provided a better understanding of the stimulation of *V. parahaemolyticus* to the physiological responses and metabolomic alterations of mud crabs, which is crucially important in prevention and control of diseases in the cultured mud crab.

Acknowledgements

The work was supported by grants from National Natural Science Foundation of China (41876152, 31850410487, 31802341), Guangdong provincial project of Science and Technology (2017B020204003), the “Sail Plan” Program for Outstanding Talents of Guangdong Province (14600605) and support from Department of Education of Guangdong Province (2017KCXTD014).

Appendix A. Supplementary data

Supplementary data to this article can be found online at https://doi.org/10.1016/j.fsi.2019.01.011.

References

[1] H.H. Ye, Y. Tao, G.Z. Wang, Q.W. Lin, X.L. Chen, S.J. Li, Experimental nursery culture of the mud crab *Scylla paramamosain* (Estampador) in China, Aquacult. Int. 19 (2011) 313–321.

[2] H.J. Wu, L.B. Sun, C.B. Li, Z.Z. Li, Z. Zhang, S.K. Li, et al., Enhancement of the immune response and protection against *Vibrio parahaemolyticus* by indigenous probiotic *Bacillus* strains in mud crab (*Scylla paramamosain*), Fish Shellfish Immunol. 41 (2014) 156–162.

[3] F.Y. Zhang, K.J. Jiang, M.M. Sun, D. Zhang, L.B. Ma, Multiplex immune-related genes expression analysis response to bacterial challenge in mud crab, *Scylla paramamosain*, Fish Shellfish Immunol. 34 (2013) 712–716.

[4] W.B. Gu, Y.L. Zhou, D.D. Tu, Z.K. Zhou, Q.H. Zhu, Y.Y. Chen, et al., Identification and characterization of pro-interleukin-16 from mud crab *Scylla paramamosain*: the first evidence of proinflammatory cytokine in crab species, Fish Shellfish Immunol. 70 (2017) 701–709.

[5] X.K. Jin, S. Li, X.N. Guo, L. Cheng, M.H. Wu, S.J. Tan, et al., Two antibacterial C-type lectins from crustacean, *Eriocheir sinensis*, stimulated cellular encapsulation in vitro, Dev. Comp. Immunol. 41 (2013) 544–552.

[6] Z.G. Shan, K.X. Zhu, H. Peng, B. Chen, J. Liu, F.Y. Chen, et al., The new antimicrobial peptide *Sp*Hyastatin from the mud crab *Scylla paramamosain* with multiple antimicrobial mechanisms and high effect on bacterial infection, Front. Microbiol. 7 (2016) 1140.

[7] H. Kumar, T. Kawai, S. Akira, Pathogen recognition in the innate immune response, Biochem. J. 420 (2009) 1–16.

[8] J. Tian, Z.J. Xie, The Na-K-ATPase and calcium-signaling microdomains, Physiology 23 (2008) 205–211.

[9] O. Aizman, A. Aperia, Na,K-ATPase as a signal transducer, Ann. Ny. Acad. Sci. 986 (2003) 489–496.

[10] Z.H. Zhuang, X.L. Zhao, H. Li, S.Y. Wang, X.X. Peng, Gut CaVP is an innate immune protein against bacterial challenge in amphioxus *Branchiostoma belcheri*, Fish Shellfish Immunol. 31 (2011) 217–223.

[11] P.F. Ji, C.L. Yao, Z.Y. Wang, Two types of calmodulin play different roles in Pacific white shrimp (*Litopenaeus vannamei*) defenses against *Vibrio parahaemolyticus* and WSSV infection, Fish Shellfish Immunol. 31 (2011) 260–268.

[12] Y.F. Ye, M.J. Xia, C.K. Mu, R.H. Li, C.L. Wang, Acute metabolic response of *Portunus trituberculatus* to *Vibrio alginolyticus* infection, Aquaculture 463 (2016) 201–208.

[13] J.K. Nicholson, J.C. Lindon, Systems biology: metabonomics, Nature 455 (2008) 1054–1056.

[14] K.A. Stringer, R.T. McKay, A. Karnovsky, B. Quemerais, P. Lacy, Metabolomics and its application to acute lung diseases, Front. Immunol. 7 (2016) 44.

[15] K.M. Sas, A. Karnovsky, G. Michailidis, S. Pennathur, Metabolomics and diabetes: analytical and computational approaches, Diabetes 64 (2015) 718–732.

[16] C.R. Evans, A. Karnovsky, M.A. Kovach, T.J. Standiford, C.F. Burant, K.A. Stringer, Untargeted LC-MS metabolomics of bronchoalveolar lavage fluid differentiates acute respiratory distress syndrome from health, J. Proteome Res. 13 (2014) 640–649.

[17] Z.Y. Du, Z.L. Shu, W. Lei, C. Li, K.W. Zeng, X.Y. Guo, et al., Integration of metabonomics and transcriptomics reveals the therapeutic effects and mechanisms of baoyuan decoction for myocardial ischemia, Front. Pharmacol. 9 (2018) 514.

[18] T.W. Collette, D.M. Skelton, J.M. Davis, J.E. Cavallin, K.M. Jensen, M.D. Kahl, et al., Metabolite profiles of repeatedly sampled urine from male fathead minnows (*Pimephales promelas*) contain unique lipid signatures following exposure to anti-androgens, Comp. Biochem. Physiol. D 19 (2016) 190–198.

[19] K.S. Solanky, I.W. Burton, S.L. MacKinnon, J.A. Walter, A. Dacanay, Metabolic changes in Atlantic salmon exposed to *Aeromonas salmonicida* detected by H-1-nuclear magnetic resonance spectroscopy of plasma, Dis. Aquat. Org. 65 (2005) 107–114.

[20] W.W. Sun, X.X. Zhang, W.S. Wan, S.Q. Wang, X.B. Wen, H.P. Zheng, et al., Tumor necrosis factor receptor-associated factor 6 (TRAF6) participates in anti-lipopolysaccharide factors (ALFs) gene expression in mud crab, Dev. Comp. Immunol. 67 (2017) 361–376.

[21] X.X. Zhang, Z.Q. Sun, X.S. Zhang, M. Zhang, S.K. Li, Hemolymph microbiomes of three aquatic invertebrates as revealed by a new cell extraction method, Appl. Environ. Microbiol. 84 (2018) e02824-17.

[22] A. Lokmer, K.M. Wegner, Hemolymph microbiome of Pacific oysters in response to temperature, temperature stress and infection, ISME J. 9 (2015) 670–682.

[23] F. Rivera-Chavez, L.F. Zhang, F. Faber, C.A. Lopez, M.X. Byndloss, E.E. Olsan, et al., Depletion of butyrate-producing *Clostridia* from the gut microbiota drives an aerobic luminal expansion of *Salmonella*, Cell Host Microbe 19 (2016) 443–454.

[24] H.T. Yang, S.S. Zou, L.J. Zhai, Y. Wang, F.M. Zhang, L.G. An, et al., Pathogen invasion changes the intestinal microbiota composition and induces innate immune responses in the zebrafish intestine, Fish Shellfish Immunol. 71 (2017) 35–42.

[25] S. Li, L. Sun, H. Wu, Z. Hu, W. Liu, Y. Li, et al., The intestinal microbial diversity in mud crab (*Scylla paramamosain*) as determined by PCR-DGGE and clone library analysis, J. Appl. Microbiol. 113 (2012) 1341–1351.

[26] J. Joshi, J. Srisala, V.H. Truong, I.T. Chen, B. Nuangsaeng, O. Suthienkul, et al., Variation in *Vibrio parahaemolyticus* isolates from a single Thai shrimp farm experiencing an outbreak of acute hepatopancreatic necrosis disease (AHPND), Aquaculture 428 (2014) 297–302.

[27] F. Han, Y. Zhang, D.L. Zhang, L.P. Liu, H.J. Tsai, Z.Y. Wang, The Rab5A gene of marine fish, large yellow croaker (*Larimichthys crocea*), and its response to the infection of *Cryptocaryon irritans*, Fish Shellfish Immunol. 54 (2016) 364–373.

[28] I. Rondon-Barragan, R. Nozaki, I. Hirono, H. Kondo, LAMP-1-chimeric DNA vaccines enhance the antibody response in Japanese flounder, *Paralichthys olivaceus*, Fish Shellfish Immunol. 67 (2017) 546–553.

[29] C.L. Brown, G. Young, R.S. Nishioka, L.C. Folmar, M. Andrews, J.R. Cashman, et al., Histopathology, blood chemistry, and physiological status of normal and moribund striped bass (*Morone saxatilis*) involved in summer mortality ('die-off') in the Sacramento—San Joaquin Delta of California, J. Fish. Biol. 44 (1994) 491–512.

[30] Q.Q. Ma, Q. Chen, Z.H. Shen, D.L. Li, T. Han, J.G. Qin, et al., The metabolomics responses of Chinese mitten-hand crab (*Eriocheir sinensis*) to different dietary oils, Aquaculture 479 (2017) 188–199.

[31] J. Na, J. Jung, J. Bang, Q. Lu, B.A. Carlson, X. Guo, et al., Selenophosphate synthetase 1 and its role in redox homeostasis, defense and proliferation, Free Radical Biol. Med. 127 (2018) 190–197.

[32] G. Chimienti, A. Picca, G. Sirago, F. Fracasso, R. Calvani, R. Bernabei, et al., Increased TFAM binding to mtDNA damage hot spots is associated with mtDNA loss in aged rat heart, Free Radical Biol. Med. 124 (2018) 447–453.

[33] B. Korzeniewski, Regulation of ATP supply during muscle contraction theoretical studies, Biochem. J. 330 (1998) 1189–1195.

[34] R.T. Zuo, M. Li, J. Ding, Y.Q. Chang, Higher dietary arachidonic acid levels improved the growth performance, gonad development, nutritional value, and antioxidant enzyme activities of adult sea urchin (*Strongylocentrotus intermedius*), J. Ocean Univ. China 17 (2018) 932–940.

[35] S. Nayak, W. Koven, I. Meiri, I. Khozin-Goldberg, N. Isakov, M. Zibdeh, et al., Dietary arachidonic acid affects immune function and fatty acid composition in cultured rabbitfish *Siganus rivulatus*, Fish Shellfish Immunol. 68 (2017) 46–53.

[36] K. Saeki, T. Yokomizo, Identification, signaling, and functions of LTB4 receptors, Semin. Immunol. 33 (2017) 30–36.

[37] S.J. Lund, A. Portillo, K. Cavagnero, R.E. Baum, L.H. Naji, J.H. Badrani, et al., Leukotriene C4 potentiates IL-33-induced group 2 innate lymphoid cell activation and lung inflammation, J. Immunol. 199 (2017) 1096–1104.

[38] B.R. Culp, W.E.M. Lands, A. Hirai, R. Gorman, Relationship of thromboxane generation to the aggregation of platelets from humans: effects of eicosapentaenoic acid, Prostaglandins 30 (1985) 819–825.

[39] M.J. Sun, J.C. Dong, Y.R. Xia, R. Shu, Antibacterial activities of docosahexaenoic acid (DHA) and eicosapentaenoic acid (EPA) against planktonic and biofilm growing *Streptococcus* mutans, Microb. Pathog. 107 (2017) 212–218.

[40] S.Y. Shin, V.K. Bajpai, H.R. Kim, S.C. Kang, Antibacterial activity of bioconverted eicosapentaenoic (EPA) and docosahexaenoic acid (DHA) against foodborne pathogenic bacteria, Int. J. Food Microbiol. 113 (2007) 233–236.

[41] G. Speziali, L. Liesinger, J. Gindlhuber, C. Leopold, B. Pucher, J. Brandi, et al., Myristic acid induces proteomic and secretomic changes associated with steatosis, cytoskeleton remodeling, endoplasmic reticulum stress, protein turnover and exosome release in HepG2 cells, J Proteomics 181 (2018) 118–130.

[42] I.R. Jung, S.E. Choi, J.G. Jung, S.A. Lee, S.J. Han, H.J. Kim, et al., Involvement of iron depletion in palmitate-induced lipotoxicity of beta cells, Mol. Cell. Endocrinol. 407 (2015) 74–84.

[43] S.W. Rabkin, P. Lodhia, Stearic acid-induced cardiac lipotoxicity is independent of cellular lipid and is mitigated by the fatty acids oleic and capric acid but not by the PPAR agonist troglitazone, Exp. Physiol. 94 (2009) 877–887.

[44] V. Spigoni, F. Fantuzzi, A. Fontana, M. Cito, E. Derlindati, I. Zavaroni, et al., Stearic acid at physiologic concentrations induces in vitro lipotoxicity in circulating angiogenic cells, Atherosclerosis 265 (2017) 162–171.

[45] K.A. Yagaloff, L. Franco, B. Simko, B. Burghardt, Essential fatty acids are antagonists of the leukotriene B4 receptor, Prostag Leukotr Ess 52 (1995) 293–297.

[46] Y.S. Huang, W.C. Huang, C.W. Li, L.T. Chuang, Eicosadienoic acid differentially modulates production of pro-inflammatory modulators in murine macrophages, Mol. Cell. Biochem. 358 (2011) 85–94.

[47] M. Shelly, B.K. Lim, L. Cancedda, S.C. Heilshorn, H.F. Gao, M.M. Poo, Local and long-range reciprocal regulation of cAMP and cGMP in axon/dendrite formation, Science 327 (2010) 547–552.

[48] M. Zaccolo, M.A. Movsesian, CAMP and cGMP signaling cross-talk: role of phosphodiesterases and implications for cardiac pathophysiology, Circ. Res. 100 (2007) 1569–1578.

[49] M. Nishiyama, A. Hoshino, L. Tsai, J.R. Henley, Y. Goshima, M. Tessier-Lavigne, et al., Cyclic AMP/GMP-dependent modulation of Ca^{2+} channels sets the polarity of nerve growth-cone turning, Nature 423 (2003) 990–995.

[50] N. Buttner, S.A. Siegelbaum, Antagonistic modulation of a hyperpolarization- activated Cl^- current in Aplysia sensory neurons by SCPB and FMRFamide, J. Neurophysiol. 90 (2003) 586–598.

[51] G.S. Wang, W.M. Nauseef, Salt, chloride, bleach, and innate host defense, J. Leukoc. Biol. 98 (2015) 163–172.

[52] A. Hempel, T. Noll, A. Muhs, H. Piper, Functional antagonism between cAMP and cGMP on permeability of coronary endothelial monolayers, Am. J. Physiol. 270 (1996) 1264–1271.

[53] M. Kool, M.A.M. Willart, M. van Nimwegen, I. Bergen, P. Pouliot, J.C. Virchow, et al., An unexpected role for uric acid as an inducer of T helper 2 cell immunity to inhaled antigens and inflammatory mediator of allergic asthma, Immunity 34 (2011) 527–540.

[54] N. Sperelakis, H. Satoh, Review of some actions of taurine on ion channels of cardiac muscle cells and others, Gen. Pharmacol. Vasc. Syst. 30 (1998) 451–463.

[55] M. Waldron, S.D. Patterson, J. Tallent, O. Jeffries, The effects of oral taurine on resting blood pressure in humans: a Meta-Analysis, Curr. Hypertens. Rep. 20 (2018) 81.

[56] Q. Wang, G.H. Zhu, D.H. Xie, W.J. Wu, P. Hu, Taurine enhances excitability of mouse cochlear neural stem cells by selectively promoting differentiation of glutamatergic neurons over GABAergic neurons, Neurochem. Res. 40 (2015) 924–931.

[57] T.L. Dutka, C.R. Lamboley, R.M. Murphy, G.D. Lamb, Acute effects of taurine on sarcoplasmic reticulum Ca^{2+} accumulation and contractility in human type I and

type II skeletal muscle fibers, J. Appl. Physiol. 117 (2014) 797–805.
[58] P. Pacher, J.S. Beckman, L. Liaudet, Nitric oxide and peroxynitrite in health and disease, Physiol. Rev. 87 (2007) 315–424.
[59] C.M. Wood, P. Part, P.A. Wright, Ammonia and urea metabolism in relation to gill function and acid-base balance in a marine elasmobranch, the spiny dogfish (*Squalus acanthias*), J. Exp. Biol. 198 (1995) 1545–1558.
[60] T.H. Sannasiddappa, G.A. Hood, K.J. Hanson, A. Costabile, G.R. Gibson, S.R. Clarke, *Staphylococcus aureus* MnhF mediates cholate efflux and facilitates survival under human colonic conditions, Infect. Immun. 83 (2015) 2350–2357.
[61] J. Kunisawa, Y. Sugiura, T. Wake, T. Nagatake, H. Suzuki, R. Nagasawa, et al., Mode of bioenergetic metabolism during B cell differentiation in the intestine determines the distinct requirement for vitamin B-1, Cell Rep. 13 (2015) 122–131.
[62] E. Spinas, A. Saggini, S.K. Kritas, G. Cerulli, A. Caraffa, P. Antinolfi, et al., Crosstalk between vitamin B and immunity, J. Biol. Regul. Homeost. Agents 29 (2015) 283–288.
[63] M.M.A. Whitten, C.J. Coates, Re-evaluation of insect melanogenesis research: views from the dark side, Pigm Cell Melanoma R 30 (2017) 386–401.
[64] J.L. Jewell, R.C. Russell, K.L. Guan, Amino acid signalling upstream of mTOR, Nat. Rev. Mol. Cell Biol. 14 (2013) 133–139.
[65] C. Ciacci, A. Manti, B. Canonico, R. Campana, G. Camisassi, W. Baffone, et al., Responses of *Mytilus galloprovincialis* hemocytes to environmental strains of *Vibrio parahaemolyticus, Vibrio alginolyticus, Vibrio vulnificus*, Fish Shellfish Immunol. 65 (2017) 80–87.